

On the
Geometric Calibration of Small-JASMINE

Wolfgang Löffler¹, Michael Biermann²

Astronomisches Rechen-Institut
am Zentrum für Astronomie der Universität Heidelberg
Mönchhofstraße 12-14, D 69120 Heidelberg

17th August 2016

¹loeffler@ari.uni-heidelberg.de

²biermann@ari.uni-heidelberg.de

Abstract

The Small-JASMINE¹ infrared astrometry mission will be complementary to previous optical astrometry missions like Hipparcos and Gaia since the near-infrared band lets Small-JASMINE observe regions like the Galactic nuclear bulge around the Galactic centre which are inaccessible in the optical bands due to strong absorption by dust. Small-JASMINE will perform the astrometry relative to Gaia foreground stars in the H_w-band with a target precision of $\sim 10 \mu\text{as}$ for the position, $\sim 20 \mu\text{as}$ for the parallax, $\sim 50 \mu\text{as/yr}$ for the proper motions and $\sim 0.007 \text{ mag}$ for the photometry. In order to achieve these targets, the satellite needs to be stable enough over timescales which are long enough so that a large-scale geometric calibration relative to Gaia and a small-scale geometric calibration relative to this can be carried out. This technical note outlines possible and feasible approaches along which these geometric calibrations can be performed with the necessary precision.

1 Brief Overview of the Instrument

As outlined by [Gouda \(2015\)](#), the Small-JASMINE instrument features

- one telescope with an aperture of 30 cm and focal length of 3.9 m
- a modified Korsch system optics with 3 mirrors and an occultation rate of 0.35
- a field of view of $0.6^\circ \times 0.6^\circ$
- a focal plane assembly with one large CMOS detector for astrometry and two smaller CMOS detectors for near-infrared photometry with active temperature control at below 180 K within $\pm 0.7 \text{ K}$
- one Teledyne H4RG-10 HgCdTe CMOS detector with 4096×4096 $10 \mu\text{m}$ ($\cong 0''.53$) pixels for H_w-band (1.1 μm – 1.7 μm) astrometry
- two Teledyne H1RG HgCdTe CMOS detectors with 1024×1024 $18 \mu\text{m}$ pixels and H- and J-band filters for photometry
- a telescope support structure made of SuperInvar with active temperature control at 278 K within $\pm 0.1 \text{ K}$
- mirrors made of CLEARCERAM-Z
- GPS with two carrier phase measurement

The characteristics of operation are

- a nominal mission length of 3 years
- a pointing satellite

¹Japan Astrometry Satellite Mission for Infrared Exploration

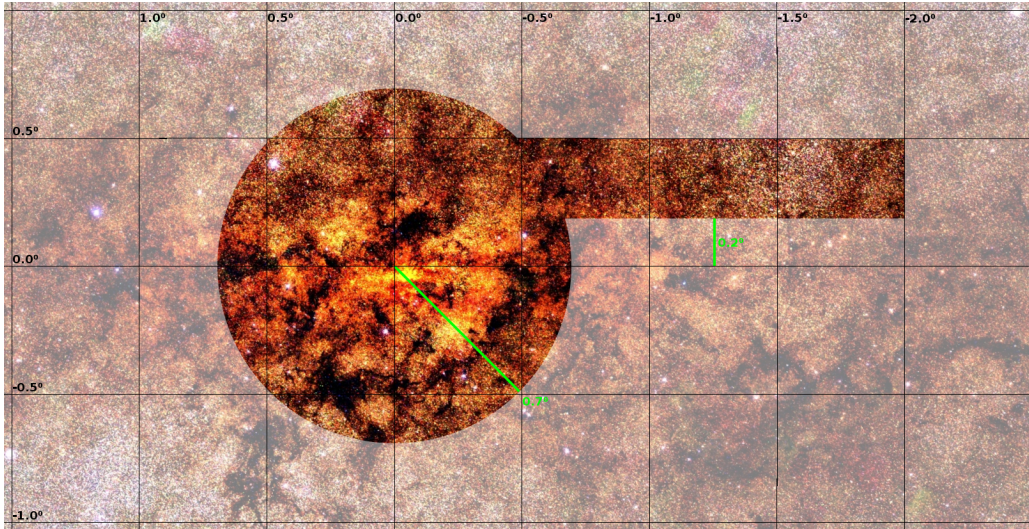


Figure 1: *The two Small-JASMINE target regions near the Galactic centre: a centred circular target with a radius of 0.7° and a rectangular off-centre target with $0.3^\circ \times 2.5^\circ$. Coloured 2MASS image.*

- a sun-synchronous orbit with an altitude higher than 550 km and LTAN² of 6:00 h resulting in an orbital period of 100 min
- two overlapping target regions, one circular region with 0.7° radius centred on ($l = 0^\circ, b = 0^\circ$) (more than 3500 target stars), one off-centre rectangular region with $0.3^\circ \times 2.5^\circ$ (more than 2000 target stars)
- observations of the target regions only while within $\pm 45^\circ$ of the vernal and autumnal equinoxes
- a detector integration time of 7.1 sec per exposure
- 20 consecutive exposures of one field of view
- 16 overlapping fields of view per orbit
- 10×10 pixel windows around each target star
- one X-band ground antenna for 10–20 Mbps data transfer

The astrometric data processing includes accurate two-dimensional centroiding within the astrometric detector windows, frame-linking of the individual fields of view, determination of J- and H-band photometry and astrometric parameters for well-behaved, i.e. apparently single and constant) stars; calibration of the point-spread functions and geometric transformations as a function of field position, time and colour. These core tasks are performed iteratively. Gaia data are used to determine the large-scale deformations of the instrument and to remove annual and secular changes in the observed field angles, i.e. to tie the relative astrometry of Small-

²Local Time of Ascending Node

JASMINE to the Gaia reference frame.

2 Physical Limits

According to [Lindgren \(2005\)](#), the angular accuracy of a single observation is limited by physics to

$$\Delta\theta \geq \frac{\sqrt{3}}{2\pi} \frac{\lambda}{D} \quad (1)$$

which corresponds to an end-of-mission accuracy limit per object of

$$\sigma \geq \frac{\sqrt{3}}{2\pi} \frac{\lambda}{D\sqrt{N}} \quad (2)$$

where λ is the wavelength of the observed photons, D the diameter of the telescope aperture and N the number of photons per object. In the case of Small-JASMINE, we have $\lambda \simeq 1.4 \mu\text{m}$, $D = 0.3 \text{ m}$ and $N = 2.5 \cdot 10^9$, resulting in

$$\Delta\theta \geq 2 \text{ mas} \quad (3)$$

for a single observation and

$$\sigma \geq 5.3 \mu\text{as} \quad (4)$$

for the end-of-mission accuracy per object. Both values are nearly a factor of two below the target centroiding accuracy of $1/150$ of a pixel for one observation, corresponding to $\sim 3.5 \text{ mas}$, and the target end-of-mission angular accuracy of $\sim 10 \mu\text{as}$.

It must be kept in mind, however, that these formulae refer to a hypothetical observation in which all the photons are used for the determination of one single astrometric parameter while, in reality, there are five astrometric parameters to be determined for every object. This will result in a decreased accuracy limit of each individual parameter even in the ideal case.

3 Calibration

The reduction by square-root law of the accuracy limit of an individual observation (c.f. Eqn. 1) to the end-of-mission accuracy limit of an object (c.f. Eqn. 2) holds only true if the errors of the individual observations are completely random, i.e. if all systematic effects have been successfully calibrated and removed from the individual measurement.

In the case of the Gaia satellite with its two telescopes and full-sky scanning, the individual measurements are not only correlated via the calibrated model of the point-spread functions and geometric transformations as a function of time, position within the field of view and colour. There exist additional correlations via the basic angle between the two telescopes and via the splines used for modelling the attitude. In the case of Small-JASMINE which is a pointing instrument with a single telescope, these latter correlations do not exist. The point-spread functions and geometric transformations from pixel coordinates to field angles are thus much easier to calibrate with fewer observations than in the case of Gaia.

3.1 Geometric Calibration

In this technical note, we will focus on possible and feasible approaches to the calibration of the geometric transformations from pixel coordinates to field angles and back, a.k.a. the geometric calibration of the instrument.

The effects which need to be calibrated stem, on the one hand, from the optical elements and the telescope structure which may introduce radially symmetric and asymmetric as well as tangential distortions of the image which vary slowly over the field of view and with colour, but may vary rather quickly in time due to mechanical and thermal effects. We will call the calibration which quantifies these kinds of effects as “large-scale geometric calibration”. On the other hand, the size and shape of individual pixels may not be uniform over the detector. According to [Beletic et al. \(2008\)](#), a 0.13 μm design process is used for the production of the H4RG-10 detector. Under the assumption that the geometric manufacturing accuracy of the detector is of the same order, each individual observation would suffer from a systematic angular uncertainty of ~ 7 mas which is thrice as large as the 2 mas physical accuracy limit of a single observation (c.f. Eq. 3).

Unless it can be demonstrated that the detector is manufactured to a geometric precision better than physical limit of a single observation, these effects must be taken into account. These detector related effects vary quickly over the field of view, i.e. from pixel to pixel, but are expected to be nearly constant over time and thus over the length of the mission. We will call this per-pixel calibration which models these effects “small-scale geometric calibration”.

Large-Scale Geometric Calibration

A possible concept for the large-scale calibration is outlined in [Godding \(1998\)](#). The formation of a point image in the image plane can thus be described as

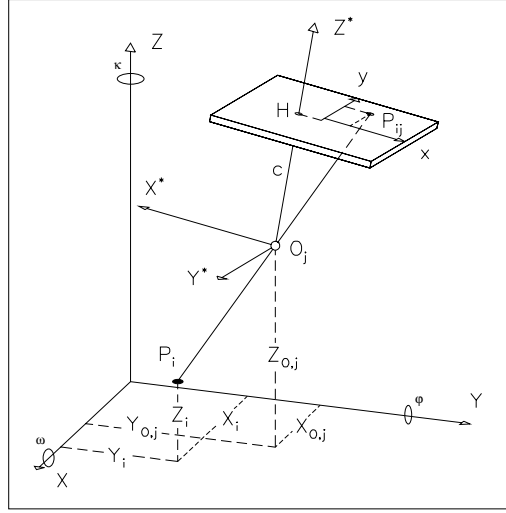


Figure 2: Principles of central perspective. The object point P_i is imaged through the perspective centre O_j to the image point P_{ij} in the image plane. H is the principal point, c (c_k in the text) is the calibrated focal length. Figure taken from [Goddard \(1998\)](#).

$$\begin{pmatrix} x_{ij} \\ y_{ij} \end{pmatrix} = -\frac{c_k}{Z_{ij}^*} \begin{pmatrix} X_{ij}^* \\ Y_{ij}^* \end{pmatrix} + \begin{pmatrix} x_H \\ y_H \end{pmatrix} + \begin{pmatrix} dx \\ dy \end{pmatrix} \quad (5)$$

with

$$\begin{pmatrix} X_{ij}^* \\ Y_{ij}^* \\ Z_{ij}^* \end{pmatrix} = D(\omega, \varphi, \kappa)_j \begin{pmatrix} X_i - X_j^O \\ Y_i - Y_j^O \\ Z_i - Z_j^O \end{pmatrix} \quad (6)$$

where X_i, Y_i and Z_i are the coordinates of an object point P_i in the object coordinate system K , $X_{O,j}, Y_{O,j}$ and $Z_{O,j}$ are the coordinates of the perspective centre O_j in the object coordinate system K , X_{ij}^*, Y_{ij}^* and Z_{ij}^* are the coordinates of the object point P_i in the object coordinate system K_j^* whose origin is fixed in O_j and whose x and y axes are parallel to the axes of the image coordinate system K_B and whose z axis is perpendicular to the image plane. x_{ij} and y_{ij} are then the coordinates of the image point P_{ij} in the image coordinate system K_B , $D(\omega, \varphi, \kappa)$ the rotation matrix between K and K_j^* , c_k the distance between the perspective centre O_j and the principal point H in the image plane, i.e. the calibrated focal length. x_H and y_H are the coordinates of the principal point H in the image coordinate system K_B . dx and dy in Equation 5 describe the large-scale distortions which must be calibrated and removed from the individual measurement.

The distortion parameters dx and dy can be expanded either in terms of orthonormal Chebychev polynomials or in terms of optical effects ([Ab-](#)

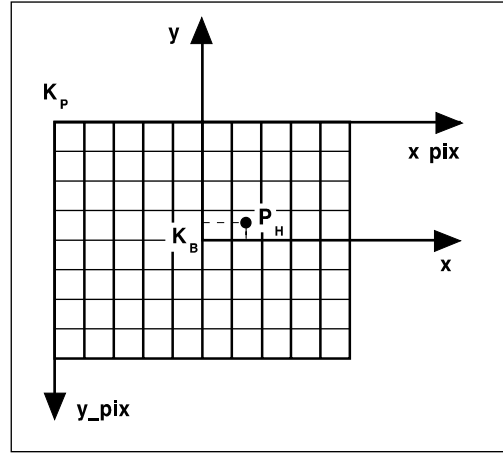


Figure 3: Definition of the image coordinate system and location of the principal point P_H . Figure taken from [Godding \(1998\)](#).

[raham & Hau 1997](#)). Expanded as Chebychev polynomials the distortion reads

$$dx = \sum_{m=0}^M \sum_{n=0}^N a_{mn} T_m(t_x x) T_n(t_y y) \quad (7)$$

$$dy = \sum_{m=0}^M \sum_{n=0}^N b_{mn} T_m(t_x x) T_n(t_y y) \quad (8)$$

with

$$T_n(x) = \cos(n \arccos(x)) \quad \text{for } -1 \leq x \leq 1 \quad (9)$$

where the parameters t_x and t_y scale the range of the image coordinates to $[-1, 1]$. Expanded in terms of optical effects the distortion is written

$$\begin{aligned} dx = & \sum_{k=1}^3 A_k (r_{ij}^{2k} - r_0^{2k}) x_{ij} \\ & + B_1 (r_{ij}^2 + 2x_{ij}) + B_2 2x_{ij} y_{ij} \\ & + C_1 x_{ij} + C_2 y_{ij} \\ & + \frac{1}{c} (D_1 (x_{ij}^2 - y_{ij}^2) + D_2 2x_{ij}^2 y_{ij}^2 + D_3 (x_{ij}^4 - y_{ij}^4)) x_{ij} \\ & + x_H \end{aligned} \quad (10)$$

$$\begin{aligned}
dy &= \sum_{k=1}^3 A_k (r_{ij}^{2k} - r_0^{2k}) y_{ij} \\
&+ B_2 (r_{ij}^2 + 2y_{ij}) + B_1 2x_{ij} y_{ij} \\
&+ \frac{1}{c} (D_1 (x_{ij}^2 - y_{ij}^2) + D_2 2x_{ij} y_{ij} + D_3 (x_{ij}^4 - y_{ij}^4)) y_{ij} \\
&+ y_H
\end{aligned} \tag{11}$$

where terms with the parameters A_k describe the radially symmetric and the terms with the parameters B_1 and B_2 the radially asymmetric and tangential distortions. The effects of affinity, i.e. skew of the coordinate axes and deviations from the image scale, are taken into consideration only in x -direction with the parameters C_1 and C_2 . Global image distortions are described by the parameters D_1 , D_2 and D_3 . x_H and y_H describe the offset of the principal point from the zero point of the image coordinates.

Whether the Chebychev or the optical expansion is used, the important points to keep in mind are that, on the one hand, all terms can be determined independently of each other by the same set of observations. On the other hand, the number of parameters to be determined is small and of the order of 20.

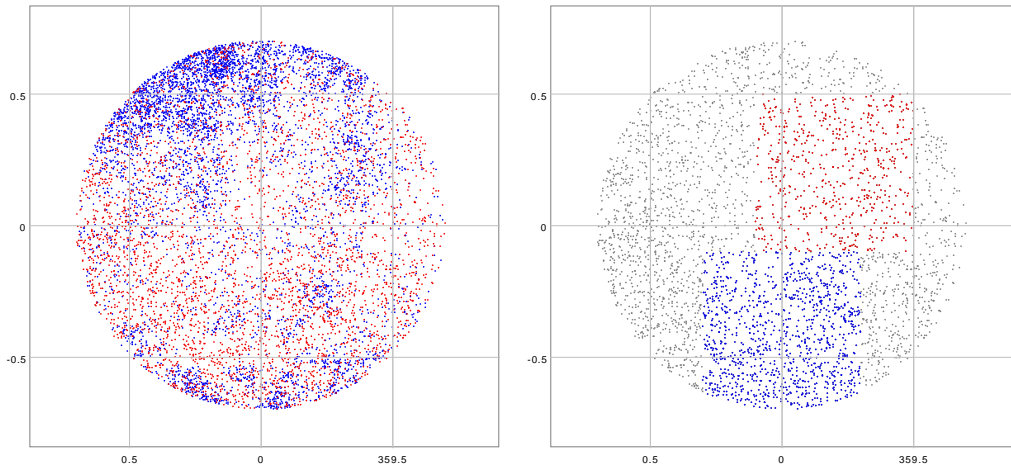


Figure 4: The circular *Small-JASMINE* target region with 8555 stars. Left: with the 4894 target stars in blue and 3661 foreground stars in red. Right: with the 3661 foreground stars in grey and two possible fields of view with 601 stars in red and 1115 stars in blue.

The left side of Figure 4 shows the circular target region around the Galactic centre containing 8555 stars with $H_w = 0.3H + 0.7J \leq 12.5$ mag and errors in H , J and K smaller than 0.2 mag. 3661 of these have a colour $J - K \leq 2.0$ and are considered to be foreground stars which are observed

by Gaia. The other 4894 stars have a colour $J - K > 2.0$ and are considered to be part of the Galactic core bulge which is not observed by Gaia.

The right side of Figure 4 shows only the foreground stars in two possible fields of view, a worst case with only 601 stars, and a best case with 1115 stars. These are the stars which can be used for the determination of the large-scale geometric calibration parameters.

Assuming that the astrometric parameters of all these stars have been determined by Gaia, assuming that Small-JASMINE and Gaia do indeed see the same object³ and finally assuming that the 20 large-scale calibration parameters to be determined are indeed orthogonal to each other, then the worst- and best-case accuracies for the large-scale calibration would be

$$\begin{aligned}\sigma_{\text{worst}} &= \frac{1}{150\sqrt{601}} \text{ pixels} = 0.27 \text{ milli-pixels} = 2.7 \text{ nm} \\ &\hat{=} 0.14 \text{ mas}\end{aligned}\tag{12}$$

$$\begin{aligned}\sigma_{\text{best}} &= \frac{1}{150\sqrt{1115}} \text{ pixels} = 0.20 \text{ milli-pixels} = 2.0 \text{ nm} \\ &\hat{=} 0.11 \text{ mas}\end{aligned}\tag{13}$$

which is more than good enough for the large-scale geometric calibration since, even in the worst-case, the calibration is better determined than the physical limit of 2 mas for a single observation (c.f. Eqn. 3).

Small-Scale Geometric Calibration

Once the large-scale geometric calibration has been successfully determined using the Gaia stars as reference, the small-scale geometric calibration must be carried out relative to the large-scale one such that both calibrations are orthogonal to each other. Essentially, the small-scale geometric calibration introduces another set of distortion terms to Equation 5 as functions of the pixel coordinates

$$dx = F_x(x, y)\tag{14}$$

$$dy = F_y(x, y) \ .\tag{15}$$

These functions F_x and F_y are continuous functions with a spatial resolution corresponding to the effective image radius which is about two pixels in the case of Small-JASMINE. No better spatially resolved information can be obtained by observations nor is it needed for calibration. These functions could, for example, be represented by splines with one node per two pixels.

³In a double star system made of a normal star and a brown dwarf, Gaia would possibly only see the normal star while Small-JASMINE would also see the brown dwarf.

At 4096×4096 pixels, we thus end up with $2048 \times 2048 = 4\,194\,304$ spatial small-scale geometric calibration units with two calibration parameters each.

Ideally, the large-scale geometric calibration removes all systematic effects which correlate pixels to each other, e.g. a skew between the pixel coordinate axes. The two small-scale geometric calibration parameters F_x and F_y on a given calibration unit are thus orthogonal to each other and can be determined independently of each other using the same observations. Furthermore, due to the relative nature of the small-scale geometric calibration, not only the foreground stars observed by Gaia can be used for the determination of the small-scale calibration parameters but all stars that are visible to Small-JASMINE.

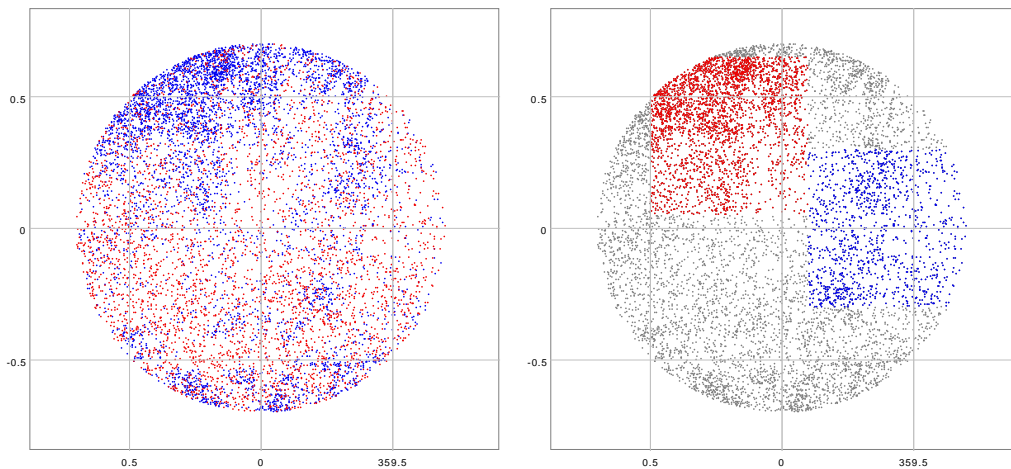


Figure 5: *The circular Small-JASMINE target region with 8555 stars. Left: with the 4894 target stars in blue and 3661 foreground stars in red. Right: with all 8555 stars in grey and two possible fields of view with 2800 stars in red and 1200 stars in blue.*

As shown in Figure 5, there are 8555 stars visible to Small-JASMINE in the circular target region around the Galactic centre. In the best fields of view, Small-JASMINE will observe up to 2800 stars, in the worst ones as few as 1200, the exact numbers depending on the detailed pointing strategy. For the sake of simplicity, we assume 2000 stars per field of view on average.

These 2000 stars will be observed 20 times per field of view. With 16 fields of view per orbit, 14 orbits per day, the Galactic centre observable for 180 days per year and a mission length of 3 years, we have

$$N_{\text{obs}} = 2000 \cdot 20 \cdot 16 \cdot 14 \cdot 180 \cdot 3 = 4\,838\,400\,000 \quad (16)$$

observations for the $4\,194\,304$ pairs of independent small-scale geometric calibration parameters – or 1153.564 observations per parameter. The accur-

acy to which a small-scale geometric calibration parameter can be determined is thus on average

$$\begin{aligned}\sigma &\simeq \frac{1}{150\sqrt{1153.564}} \text{ pixels} = 0.20 \text{ milli-pixels} = 2.0 \text{ nm} \\ &\hat{=} 0.10 \text{ mas}\end{aligned}\tag{17}$$

which is much better than the physical accuracy limit of 2 mas for a single observation (c.f. 3) – albeit under the assumption that the detector geometry does not evolve over the three years of the mission and the small-scale geometric calibration stays constant.

If we were to split the mission length into 360 temporal small-scale geometric calibration units of equal length, we would have 13 440 000 observations for the 4 194 304 pairs of small-scale geometric calibration parameters per spatial unit – or 3.204 observations per parameter. The resulting accuracy of the small-scale geometric calibration parameters in one temporal calibration unit would then be

$$\begin{aligned}\sigma &\simeq \frac{1}{150\sqrt{3.204}} \text{ pixels} = 3.72 \text{ milli-pixels} = 37.2 \text{ nm} \\ &\hat{=} 1.97 \text{ mas}\end{aligned}\tag{18}$$

which is of the same order as the physical accuracy limit of 2 mas for a single observation. The theoretical lower limit for the time length of a temporal small-scale calibration unit under these simplified assumptions is thus 36 hours.

The more realistic minimum time-length of such a calibration unit is, however, much longer. The number of 2000 observations per field of view is an average value. The distribution of the stars on the sky is not even, the pointing of the telescope not perfectly systematic. At the end of such a short temporal calibration unit, some spatial calibration units could thus be covered by many more than three observations while others would not be covered by any observation at all. Even if all spatial calibration units were covered by enough observations, it could happen that these observations are not well connected to the rest of the problem and thus lead to null sub-spaces in the overall solution space. The overall mathematical problem would then be degenerate and the numerical solution of the astrometric problem would run the risk of being unphysical.

In order to find the realistic length of the temporal small-scale geometric calibration unit and to make sure that the overall mathematical problem including the small-scale geometric calibration is non-degenerate and sufficiently well conditioned, a careful investigation of the observations process

by the Small-JASMINE satellite and corresponding data reduction is advisable. This can most easily and reliably be done by a sufficiently realistic simulation.

Additional Calibration Observations

Small-JASMINE will observe the Galactic centre only around the vernal and autumnal equinox. During summer and winter, other targets will be observed. These observations will, as long as it will be possible to carry out the corresponding large-scale geometric calibration using Gaia stars, also contribute to the small-scale geometric calibration and better conditioning of the mathematical problem.

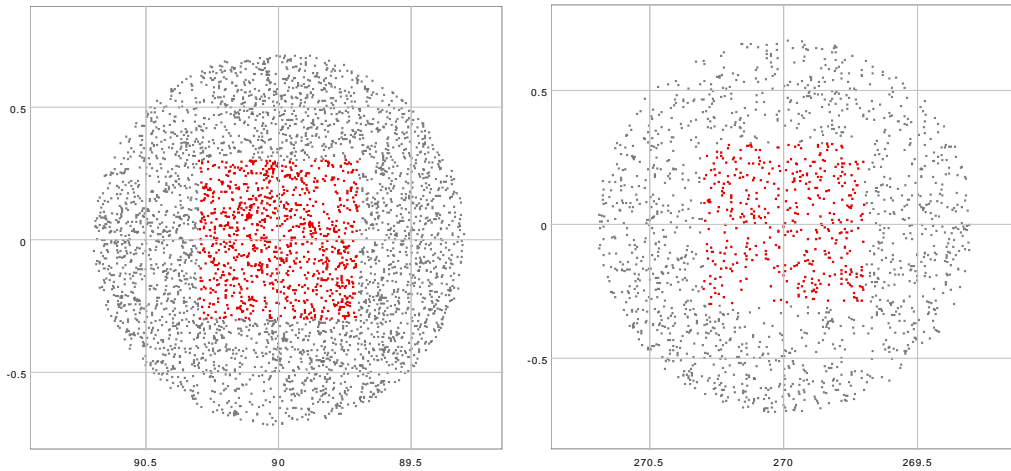


Figure 6: Possible Small-JASMINE fields of view in the Galactic plane. Left: at $\ell = 90^\circ$ with 974 stars. Right: at $\ell = 270^\circ$ with 412 stars.

Figure 6 shows two possible fields of view in the Galactic plane, one at $\ell = 90^\circ$, the other one at $\ell = 270^\circ$. The numbers of 974 and 412 stars, respectively, are rather small compared to those in the Galactic centre and would thus not contribute significantly to the small-scale geometric calibration or conditioning of the mathematical problem. Other random fields in the Galaxy will very likely suffer from the same problem.

Figure 7 shows two more possible fields of view on the two largest globular star clusters of our Galaxy, ω Centauri and 47 Tucanae with 2830 and 1801 stars, respectively. Observations of these star clusters would thus contribute to the small-scale geometric calibration in a similar manner as the observations of the Galactic centre. However, of these two star clusters, only 47 Tucanae is suitably located on the sky for off-season observations.

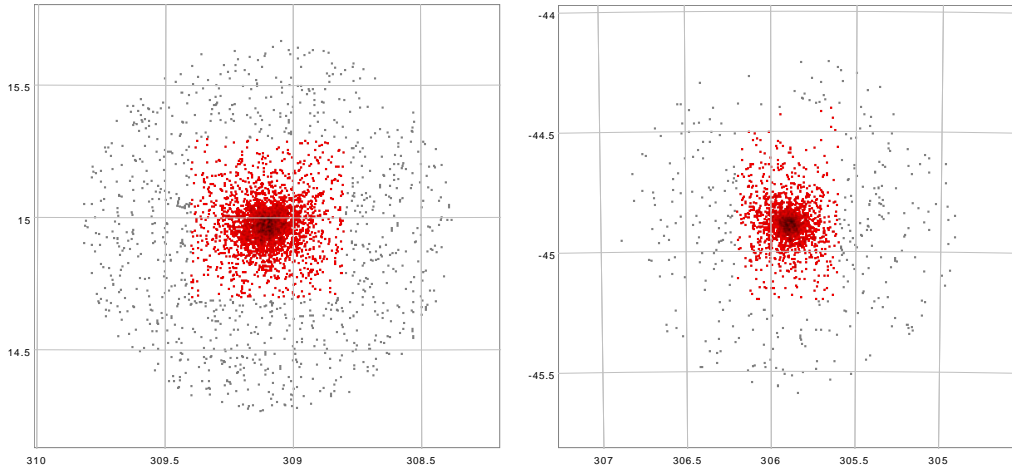


Figure 7: Possible Small-JASMINE fields of view on globular star clusters. Left: ω Centauri with 2830 stars. Right: 47 Tucanae with 1801 stars.

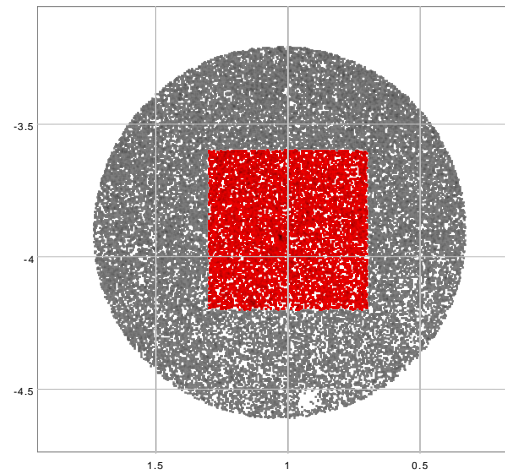


Figure 8: Possible Small-JASMINE field of view on Baade's window with 9201 stars.

Figure 8 finally shows another possible field of view on Baade's window, located close to the Galactic centre, with 9201 stars.

Spending some on-season time for observing ω Centauri and Baade's window as well as some off-season time for observing 47 Tucanae could possibly contribute to a more even coverage of the spatial small-scale calibration units with observations and thus possibly lead to a better conditioning of the overall mathematical problem.

In closing we wish to mention that an iteration between the larger-scale and small-scale calibration steps will be necessary to allow the Small-JASMINE target objects which are not observed by Gaia to fully contribute

to the geometric calibration problem.

4 Conclusions

We have shown that the Small-JASMINE mission as described in [Gouda \(2015\)](#) can determine the large-scale geometric calibration of the optics for each individual field of view as well as the more or less time-independent small-scale geometric calibration of the detector to a precision better than the physical accuracy limit of one single observation. This means that the uncertainty of a single observation is dominated by random noise and not by systematics. Since, contrary to the case of Gaia where the observations are correlated over time via the attitude and basic angle, the individual observations of Small-JASMINE are not correlated, the errors in the calibrations will thus also be uncorrelated and therefore cancel out with increasing number of observations. This means that the accuracy limit of an individual observation can, if the astrometric and calibration unknowns are well connected and the mathematical problem well conditioned, reduce to the end-of-mission accuracy limit with the square root of the number of observations.

If pre-launch investigations of the Teledyne H4RG-10 detector should indicate a secular time-evolution of its small-scale geometry at pixel level, this evolution could still be calibrated to sufficient precision under the assumption that the small-scale geometry stays more or less constant over a few days to weeks.

The assumptions inherent to this calibration model are that all geometric calibrations are orthogonal to each other and can thus be determined independently using the same observations. This means that there must not exist any other uncalibrated correlations which would invalidate the arguments above. A possible source of such uncalibrated correlations could be the modelling of the point-spread functions used to determine the centroid of an individual observation. The correct calibration of these point-spread functions is, however, a separate task whose discussion is beyond the scope of this technical note.

Acknowledgements

We would like to thank U. Bastian for valuable insight and discussions.

Bibliography

Abraham S., Hau T., 1997, In: El-Hakim S.F. (ed.) Videometrics V, Proc. of SPIE Vol. 3174, 82–93, SPIE, San Diego

Beletic J.W., Blank R., Gulbransen D., et al., 2008, In: Dorn D.A., Holland A.D. (eds.) High Energy, Optical, and Infrared Detectors for Astronomy III, Proc. of SPIE Vol. 7021, 1–14, SPIE, Marseille

Godding R., 1998, AICON 3D Systems GmbH, URL www.falcon.de/falcon/pdf/en/aicon/geometric_calibration.pdf

Gouda N., 2015, IAU General Assembly, 22, URL https://www.iau.org/static/science/scientific_bodies/divisions/a/2015/da_naoteru_gouda_astronomy.ppt

Lindgren L., 2005, In: Turon C., O’Flaherty K.S., Perryman M.A.C. (eds.) Proceedings of the Gaia Symposium "The Three-Dimensional Universe with Gaia", 29–34, ESA Special Publication SP-576